Journal of Nonlinear Modeling and Analysis
Volume 1, Number 1, March 2019, 107–128
http://jnma.ca; http://jnma.ijournal.cn
DOI:10.12150/jnma.2019.107

Dynamics and Bifurcation Study on an Extended Lorenz System

Pei Yu[1], Maoan Han[2,3,†] and Yuzhen Bai[4]

Abstract In this paper, we study dynamics and bifurcation of limit cycles in a recently developed new chaotic system, called extended Lorenz system. A complete analysis is provided for the existence of limit cycles bifurcating from Hopf critical points. The system has three equilibrium solutions: a zero one at the origin and two non-zero ones at two symmetric points. It is shown that the system can either have one limit cycle around the origin, or three limit cycles enclosing each of the two symmetric equilibria, giving a total six limit cycles. It is not possible for the system to have limit cycles simultaneously bifurcating from all the three equilibria. Simulations are given to verify the analytical predictions.

Keywords Lorenz system, extended Lorenz system, Hopf bifurcation, limit cycle, normal form.

MSC(2010) 34C07, 34C23, 34C45.

1. Introduction

Bifurcation of limit cycles has been extensively studied in planar vector fields, for example see the review article [10] and books [4,5], as well as the references therein. This problem is closely related to the well-known Hilbert's 16th problem [6]. The second part of Hilbert's 16th problem is to find an upper bound on the number of limit cycles that planar polynomial systems can have. This number is called Hilbert number, denoted by $H(n)$, where n is the degree of the polynomials. A modern version of this problem was later formulated by Smale, chosen as one of his 18 most challenging mathematical problems for the 21st century [20]. So far, for quadratic systems, the best result is $H(2) \geq 4$, obtained almost 40 years ago [1, 18, 19], but $H(2) = 4$ is still open. For cubic systems, many results have been obtained on the lower bound of $H(3)$, with the best result obtained so far as $H(3) \geq 13$ [9, 11].

On the other hand, Hopf bifurcation [7] has been applied for considering bifurcation of limit cycles from equilibria for a long time, for example see [15], and many

[†]the corresponding author.
Email address:pyu@uwo.ca (P. Yu), mahan@shun.edu.cn (M. Han), baiyu99@126.com (Y. Bai)
[1]Department of Applied Mathematics, Western University, London, Ontario N6A 5B7, Canada
[2]Department of Mathematics, Zhejiang Normal University, Jinhua, Zhejiang 321004, China
[3]Department of Mathematics, Shanghai Normal University, Shanghai 200234, China
[4]School of Mathematical Sciences, Qufu Normal University, Qufu, shandong 273165, China

physical examples can be found, for example in [5]. Recently, particular attention was paid to some 3-dimensional dynamical systems, e.g., see [2, 12, 26]. On the other hand, in the past two decades, many chaotic systems have been constructed to study chaos control and chaos synchronization. However, in order to achieve the two goals, the dynamics of the system such as stability and bifurcation must be explored. Among those systems, the family of Lorenz system [13] is an important class of chaotic systems to be studied. Thus, investigating systems which are similar to the Lorenz family yet not equivalent to Lorenz family is certainly very interesting and of importance for theoretical studies. In fact, a so-called extended Lorenz system was developed in [16] to study chaotic dynamics, which is described by

$$\begin{aligned} \dot{x} &= y, \\ \dot{y} &= m\,x - n\,y - m\,xz - p\,x^3, \\ \dot{z} &= -\,a\,z + b\,x^2, \end{aligned} \tag{1.1}$$

where m, n, p, a and b are real parameters. It can be shown that using the following transformation:

$$\begin{aligned} &x = \sqrt{2}\,X, \quad y = \sqrt{2}\big(X + \tfrac{Y}{\sigma}\big), \quad z = \tfrac{X^2}{\sigma} + (\rho - 1)\,Z, \\ &a = -\,r, \quad b = \tfrac{2\sigma - r}{\sigma(\rho - 1)}, \quad m = \sigma(\rho - 1), \quad p = 1, \quad n = \sigma + 1, \end{aligned} \tag{1.2}$$

system (1.1) can be transformed to the standard Lorenz system:

$$\begin{aligned} \dot{X} &= \sigma(Y - X), \\ \dot{Y} &= \rho\,X - Y - XZ, \\ \dot{Z} &= -\,r\,Z + XY. \end{aligned} \tag{1.3}$$

However, it should be noted in (1.2) that p is particularly taken as 1, and so in general the two systems (1.1) and (1.3) are not topologically equivalent. In fact, we will see in the next section that system (1.1) can have more limit cycles than that system (1.3) can. Therefore, in this paper, particular attention is paid to the original system (1.1). Note that both the extended Lorenz system (1.1) and the classical Lorenz system (1.3) are invariant under the transformation: $(x, y, z) \to (-x, -y, z)$. Hence, solution trajectories of these two systems are symmetric with the z-axis. Also, note that the z-axis (or Z-axis for the classical Lorenz system) is an invariant manifold. Trajectories starting from the z-axis (or Z-axis for the classical Lorenz system) either converges to the origin if $a > 0$ or diverges to $\pm\infty$ if $a < 0$.

Hopf bifurcation for the classical Lorenz system (1.3) has been studied by many authors. In particular, Pade *et al.* [17] applied the center manifold theory and averaging method to prove that the Hopf bifurcation is subcritical for $r > 0$ and $\sigma > r + 1$. This implies that for the classical Lorenz system, only two limit cycles (with 1-1 distribution) can bifurcate from the two symmetric equilibria, which contradicts the existence of six limit cycles (with 3-3 distribution) shown in [23]. Hopf bifurcation was also considered for the Chen [8, 14] and Lü [27, 28] chaotic systems (which belong to the so called Lorenz family), but no attention was paid to multiple limit cycle bifurcations in these articles.

In the next section, we first briefly present the method of normal forms and its computation for analyzing Hopf bifurcation and multiple limit cycle bifurcation. Then, in order to make a comparison between the extended Lorenz system (1.1) and the classical Lorenz system (1.3), we applied normal form theory to consider limit cycles bifurcating in the classical Lorenz system (1.3) due to Hopf bifurcation, and our result confirms that obtained by Pade [17]. The main result for the extended Lorenz system (1.1) is then obtained by using the same normal form method, which proves the existence of six (with 3-3 distribution) limit cycles. Simulations to verify the analytical predictions are given in Section 3, and finally conclusion is drawn in Section 4.

2. Main results

2.1. Methodology

In this paper, the method of normal forms will be applied to consider systems (1.1) and (1.3). Suppose for general nonlinear dynamical system, $\dot{x} = f(x, \mu)$, $x \in R^n$, $\mu \in R^k$, $f(0, \mu) = 0$ and assume the system has a Hopf critical point at $(x, \mu) = (0, 0)$. The normal form can be obtained using computer algebra systems (e.g., see [21, 22, 24]) as given in polar coordinates:

$$\begin{aligned} \dot{r} &= r\left(v_0 + v_1 r^2 + v_2 r^4 + \cdots + v_k r^{2k} + \cdots\right), \\ \dot{\theta} &= \omega_c + \tau_0 + \tau_1 r^2 + \tau_2 r^4 + \cdots + \tau_k r^{2k} + \cdots, \end{aligned} \tag{2.1}$$

where r and θ represent the amplitude and phase of motion, respectively. v_k $(k = 0, 1, 2, \cdots)$ is called the kth-order focus value. v_0 and τ_0 are obtained from linear analysis. The first equation of (2.1) can be used for studying bifurcation of limit cycles and stability of bifurcating limit cycles. To find k small-amplitude limit cycles bifurcating from the origin, we first solve the k parametric equations: $v_0 = v_1 = \cdots = v_{k-1} = 0$ such that $v_k \neq 0$, and then perform appropriate small perturbations to prove the existence of k limit cycles. The following Lemma gives sufficient conditions for proving the existence of k small-amplitude limit cycles. (The proofs can be found in [25].)

Lemma 2.1. *Suppose that the focus values for the general dynamical system $\dot{x} = f(x, \mu)$ are given such that $v_j = v_j(\mu)$, $j = 0, 1, \ldots, k$, satisfying $v_j(\mu_c) = 0$, $j = 0, 1, \ldots, k-1$, $v_k(\mu_c) \neq 0$ and*

$$\operatorname{rank}\left[\frac{\partial(v_0, v_1, \ldots, v_{k-1})}{\partial(\mu_1, \mu_2, \ldots, \mu_k)}\right]_{\mu=\mu_c} = k.$$

Then, for any given μ near μ_c, the dynamical system can have at most k small limit cycles bifurcating from the origin; and for some μ near μ_c, the system can have k limit cycles around the origin.

2.2. Limit cycle bifurcation in the classical Lorenz system (1.3)

The classical chaotic Lorenz system (1.3) has three equilibria:

$$\begin{aligned} &\mathrm{C}_0 : \ (0,0,0), \quad \text{for any parameter values,} \\ &\mathrm{C}_\pm : \big(\pm\sqrt{r(\rho-1)}, \pm\sqrt{r(\rho-1)}, \rho-1\big), \quad \text{for} \ \ \rho \geq 1. \end{aligned} \tag{2.2}$$

The stability can be obtained from the Jacobian of the system evaluated at the equilibria. The characteristic polynomial for the C_0 is

$$P_{\mathrm{C}_0}(\lambda) = (\lambda + r)[\lambda^2 + (\sigma+1)\,\lambda + (1-\rho)\,\sigma]. \tag{2.3}$$

According to the physical meaning, all the parameters in (1.3) take positive values. Thus, the trivial equilibrium C_0 is asymptotically stable for $0 < \rho < 1$ for which the symmetric equilibria $\mathrm{C}_\pm$ do not exist. Moreover, it can be shown using Lyapunov function that the C_0 is globally asymptotically stable for $0 < \rho \leq 1$ ($\sigma > 0$, $r > 0$) (e.g., see [3]). When $\rho > 1$, the C_0 becomes unstable and the $\mathrm{C}_\pm$ exist, whose stability is determined by the following characteristic polynomial:

$$P_{\mathrm{C}_\pm}(\lambda) = \lambda^3 + (\sigma + r + 1)\,\lambda^2 + r(\sigma+\rho)\,\lambda + 2\sigma r(\rho-1), \tag{2.4}$$

indicating that the $\mathrm{C}_\pm$ are asymptotically stable for

$$\rho > 1 \quad \text{and} \quad (r+1-\sigma)\,\rho + (\sigma + r + 3)\,\sigma > 0. \tag{2.5}$$

Therefore, the equilibria $\mathrm{C}_\pm$ are always stable for $r + 1 - \sigma \geq 0$. If $\sigma > r + 1$, there exists a Hopf critical point, defined by

$$\rho_{\mathrm{H}} = \frac{(\sigma + r + 3)\,\sigma}{\sigma - r - 1}, \quad (\sigma > r + 1). \tag{2.6}$$

Then, the $\mathrm{C}_\pm$ are asymptotically stable for $1 < \rho < \rho_{\mathrm{H}}$, and becomes unstable for $\rho > \rho_{\mathrm{H}}$. A Hopf bifurcation occurs from the $\mathrm{C}_\pm$ at $\rho = \rho_{\mathrm{H}}$.

In the following, we investigate the limit cycles bifurcating from the $\mathrm{C}_\pm$ due to Hopf bifurcation at the critical point $\rho = \rho_{\mathrm{H}}$ under the conditions $r > 0$ and $\sigma > r + 1$. Note that when $\rho = \rho_{\mathrm{H}}$, the system still has two free parameters σ and r, which implies that there may exist maximal 3 limit cycles around each of the $\mathrm{C}_\pm$. However, surprisingly we have the following result.

Theorem 2.1. *When $r > 0$, $\sigma > r + 1$, $\rho > 1$, Hopf bifurcation can occur from the stable equilibria $\mathrm{C}_\pm$ at the critical point $\rho = \rho_{\mathrm{H}}$. The maximal number of small limit cycles around each of the $\mathrm{C}_\pm$ is one. Thus, the total maximal number of limit cycles bifurcating from the symmetric equilibria $\mathrm{C}_\pm$ is two, and the bifurcating limit cycles are unstable, i.e. the Hopf bifurcation is subcritical.*

Proof. Suppose $r > 0$, $\sigma > r + 1$ and let $\rho = \rho_{\mathrm{H}}$. Then, introducing the transformation:

$$\begin{pmatrix} X \\ Y \\ Z \end{pmatrix} = \begin{pmatrix} \sqrt{r(\rho-1)} \\ \sqrt{r(\rho-1)} \\ \rho - 1 \end{pmatrix} + T_1 \begin{pmatrix} u \\ v \\ w \end{pmatrix}, \tag{2.7}$$

where

$$T_1 = \begin{bmatrix} \frac{\sigma(\sigma-r-1)}{\sigma^2-1}\,\bar{T} & \frac{(\sigma-r-1)^2\,\omega_{C_\pm}}{2r(\sigma^2-1)}\,\bar{T} & \frac{\sigma}{r}\,\bar{T} \\ \frac{\sigma-r-1}{\sigma^2-1}\,\bar{T} & \frac{(\sigma+r-1)(\sigma-r-1)\,\omega_{C_\pm}}{2r(\sigma^2-1)}\,\bar{T} & \frac{r+1}{r}\,\bar{T} \\ 1 & 0 & 1 \end{bmatrix}, \tag{2.8}$$

with $\bar{T} = \sqrt{r(\sigma+1)/(\sigma+r+1)/(\sigma-r-1)}$, into (1.3), we obtain the system:

$$\begin{aligned} \dot{u} &= \omega_{C_\pm}\, v + \textstyle\sum_{i+j+k=2}^{3} A_{ijk} u^i v^j w^k, \\ \dot{v} &= -\,\omega_{C_\pm}\, u + \textstyle\sum_{i+j+k=2}^{3} B_{ijk} u^i v^j w^k, \\ \dot{w} &= -\,(\sigma+r+1)\, w + \textstyle\sum_{i+j+k=2}^{3} C_{ijk} u^i v^j w^k, \end{aligned} \tag{2.9}$$

where $\omega_{C_\pm} = \sqrt{2\sigma r(\sigma+1)/(\sigma-r-1)}$, A_{ijk}, B_{ijk} and C_{ijk} are coefficients expressed in terms of σ and r. Let $\sigma = r+1+\tilde{\sigma}$. Then $\sigma > r+1$ is equivalent to $\tilde{\sigma} > 0$. Now applying the Maple program [24] to system (2.9) we obtain the first focus value v_1 as follows:

$$v_1 = \frac{\tilde{\sigma}^2(\tilde{\sigma}+r+1)}{16(\tilde{\sigma}+r)(\tilde{\sigma}+r+2)(\tilde{\sigma}+2r+2)}\,\frac{F_1}{F_0},$$

where F_0 and F_1 are given by

$$\begin{aligned} F_0 =& \big[\tilde{\sigma}^3 + 2(3r+2)\tilde{\sigma}^2 + 2(4r^2+7r+2)\tilde{\sigma} + 2r(r+1)(r+2)\big]^2 \\ &\times \big[2\tilde{\sigma}^3 + (7r+9)\tilde{\sigma}^2 + (9r^2+20r+12)\tilde{\sigma} + (r+1)(r+2)(3r+2)\big] \\ &\times \big[4\tilde{\sigma}^9 + 52(r+1)\tilde{\sigma}^8 + (325r^2+582r+289)\tilde{\sigma}^7 + (1206r^3+3066r^2+2716r+892)\tilde{\sigma}^6 \\ &+ (2743r^4+9336r^3+11670r^2+6800r+1660)\tilde{\sigma}^5 + (3818r^5+16786r^4+27912r^3 \\ &+ 22720r^2+9760r+1888)\tilde{\sigma}^4 + (3181r^6+17482r^5+37309r^4+39920r^3+23520r^2 \\ &+ 7904r+1264)\tilde{\sigma}^3 + 4(r+1)(r+2)(375r^5+1376r^4+1743r^3+986r^2+324r+56)\tilde{\sigma}^2 \\ &+ 4(r+1)^2(r+2)^2(89r^4+166r^3+69r^2+20r+4)\tilde{\sigma} + 32r^3(r+1)^3(r+2)^3\big], \end{aligned}$$

$$\begin{aligned} F_1 =& 4\tilde{\sigma}^{17} + 4(27r+26)\tilde{\sigma}^{16} + (1427r^2+2608r+1253)\tilde{\sigma}^{15} + (11551r^3+31889r^2+29013r \\ &+ 9273)\tilde{\sigma}^{14} + (62828r^4+238722r^3+326079r^2+196936r+47104)\tilde{\sigma}^{13} \\ &+ (242358r^5+1199652r^4+2240085r^3+2018637r^2+910506r+173800)\tilde{\sigma}^{12} \\ &+ (687176r^6+4266776r^5+10306431r^4+12611736r^3+8434430r^2+3030478r \\ &480656)\tilde{\sigma}^{11} + (1470972r^7 + 11117378r^6 + 33425981r^5 + 52566837r^4 \\ &+ 47417128r^3 + 25098194r^2 + 7481232r + 1013232)\tilde{\sigma}^{10} \\ &+ (2430245r^8 + 21749170r^7 + 78924719r^6 + 153489738r^5 + 176826526r^4 \\ &+ 125364038r^3 + 54683844r^2 + 13903032r + 1638912)\tilde{\sigma}^9 \\ &+ (3154149r^9 + 32524303r^8 + 138601237r^7 + 323266785r^6 + 457910872r^5 \\ &+ 412045718r^4 + 238969280r^3 + 88295040r^2 + 19529664r + 2030336)\tilde{\sigma}^8 \\ &+ (3247504r^{10} + 37579700r^9 + 183373802r^8 + 499553970r^7 + 844428866r^6 \end{aligned}$$

$$
\begin{aligned}
&+ 929336154r^5 + 679634260r^4 + 331181216r^3 + 105686400r^2 \\
&+ 20627904r + 1906432)\tilde{\sigma}^7 + (2642920r^{11} + 33561998r^{10} + 183410712r^9 \\
&+ 570316548r^8 + 1121914168r^7 + 1467244998r^6 + 1305390840r^5 + 796312152r^4 \\
&+ 332070272r^3 + 92802496r^2 + 16138496r + 1328896)\tilde{\sigma}^6 \\
&+ 2(r+2)(r+1)(832651r^{10} + 8929440r^9 + 40286202r^8 + 100663780r^7 \\
&+ 154067167r^6 + 150972284r^5 + 96648684r^4 + 40896688r^3 + 11487232r^2 \\
&+ 2026176r + 165888)\tilde{\sigma}^5 + 2(r+2)^2(r+1)^2(391199r^9 + 3410791r^8 \\
&+ 12144161r^7 + 23043333r^6 + 25525592r^5 + 17157628r^4 + 7227504r^3 \\
&+ 2006240r^2 + 357952r + 27904)\tilde{\sigma}^4 + 4(r+2)^3(r+1)^3(64931r^8 + 438311r^7 \\
&+ 1153923r^6 + 1518369r^5 + 1075554r^4 + 433768r^3 + 115704r^2 + 20976r + 1408)\tilde{\sigma}^3 \\
&+ 8(r+2)^4(r+1)^4(7057r^7 + 34285r^6 + 59607r^5 + 45287r^4 + 15944r^3 \\
&+ 3892r^2 + 736r + 32)\tilde{\sigma}^2 + 16r(r+2)^5(r+1)^5(443r^5 + 1353r^4 + 1185r^3 + 275r^2 \\
&+ 56r + 12)\tilde{\sigma} + 128r^4(r+2)^6(r+1)^6(3r+4).
\end{aligned}
$$

It is obvious that for $r > 0$ and $\tilde{\sigma} > 0$, $F_0 > 0$ and $F_1 > 0$, and so $v_1 > 0$ for $r > 0$ and $\sigma > r + 1$, implying that the Hopf bifurcation is subcritical and the bifurcating limit cycle is unstable.

This completes the proof of Theorem 2.1. □

Theorem 2.1 confirms the result obtained by Pade *et al.* [17].

2.3. Stability and bifurcation of equilibria of the extended Lorenz system (1.1)

Now, we study the extended Lorenz system (1.1). First, it is easy to find that this system also has three equilibria, given by

$$
\begin{aligned}
&\mathrm{E}_0 : \ (0,0,0), \quad \text{for any parameter values,} \\
&\mathrm{E}_\pm : \left(\pm\sqrt{\tfrac{am}{ap+bm}},\ 0,\ \tfrac{bm}{ap+bm}\right), \quad \text{for} \quad \tfrac{am}{ap+bm} \geq 0 \ \text{ and } \ ap + bm \neq 0.
\end{aligned} \tag{2.10}
$$

The stability of the equilibria is determined by the Jacobian of the system,

$$
J(x,y,z) = \begin{bmatrix} 0 & 1 & 0 \\ m - mz - 3px^2 & -n & -mx \\ 2bx & 0 & -a \end{bmatrix}. \tag{2.11}
$$

Thus, evaluating J at the E_0 gives

$$
J(\mathrm{E}_0) = \begin{bmatrix} 0 & 1 & 0 \\ m & -n & 0 \\ 0 & 0 & -a \end{bmatrix}, \tag{2.12}
$$

which yields the characteristic polynomial:

$$
P_{\mathrm{E}_0}(\lambda) = (\lambda + a)(\lambda^2 + n\lambda - m) = \lambda^3 + (a+n)\lambda^2 + (an - m)\lambda - am, \tag{2.13}
$$

indicating that the E_0, which exists for any real parameter values, is asymptotically stable if

$$a > 0, \quad m < 0 \quad \text{and} \quad n > 0. \tag{2.14}$$

Note that when $a < 0$, $P_{\mathrm{E}_0}(\lambda)$ has a positive eigenvalue, implying that even a stable limit cycle, embedded in a two-dimensional center manifold, would be actually unstable in the whole system. Since in this paper attention is focused on Hopf bifurcation, we will assume $a > 0$ when we explore Hopf bifurcation from the equilibrium E_0.

Similarly, evaluating J at the $\mathrm{E}_\pm$ results in

$$J(\mathrm{E}_\pm) = \begin{bmatrix} 0 & 1 & 0 \\ -\frac{2map}{ap+bm} & -n & \mp m\sqrt{\frac{am}{ap+bm}} \\ \pm 2b\sqrt{\frac{am}{ap+bm}} & 0 & -a \end{bmatrix}, \tag{2.15}$$

which in turn gives the characteristic polynomial:

$$P_{\mathrm{E}_\pm}(\lambda) = \lambda^3 + (a+n)\lambda^2 + a\big(n + \tfrac{2mp}{ap+bm}\big)\,\lambda + 2am, \tag{2.16}$$

implying that the $\mathrm{E}_\pm$ are asymptotically stable if the following conditions hold:

$$am > 0, \quad a+n > 0 \quad \text{and} \quad a\big[(a+n)\big(n + \tfrac{2mp}{ap+bm}\big) - 2m\big] > 0. \tag{2.17}$$

Note that stable $\mathrm{E}_\pm$ can exist for both $a > 0$ and $a < 0$, described as follows: $\mathrm{E}_\pm$ are asymptotically stable when

$$\begin{aligned} &a>0, m>0,\ a+n>0, \begin{cases} \text{Case I:} \quad b > -\frac{a}{m}\,p, \ \text{ if } \ 0<m<\frac{1}{2}(a+n)n, \ n>0; \\ \text{Case II:} \quad -\frac{a}{m}p < b \le \big[\frac{2(a+n)}{2m-(a+n)n} - \frac{a}{m}\big]p, \ p>0, \\ \qquad\qquad\qquad \text{if } \ m>\max\big\{0, \tfrac{1}{2}(a+n)n\big\}; \end{cases} \\ &a<0, m<0,\ a+n>0, \qquad \text{Case III:} \ \ \big[\tfrac{2(a+n)}{2m-(a+n)n} - \tfrac{a}{m}\big]p \le b < -\tfrac{a}{m}\,p, \ p>0, \\ &\qquad\qquad\qquad\qquad\qquad\qquad\qquad\qquad \text{if } \ m<\max\big\{0, \tfrac{1}{2}(a+n)n\big\}. \end{aligned} \tag{2.18}$$

Firstly, it is easy to see by comparing the equations (2.13) and (2.16) that there exists a pitchfork bifurcation between the E_0 and $\mathrm{E}_\pm$ at the critical point, defined by $am = 0$.

Secondly, we consider possible Hopf bifurcations arising from the equilibria E_0 and $\mathrm{E}_\pm$. For the E_0, it is straightforward to find the Hopf critical point at $n = 0$ ($a > 0$, $m < 0$) with the critical frequency $\omega_{\mathrm{E}_0} = \sqrt{-m}$ ($m < 0$). Next, consider Hopf bifurcation from the $\mathrm{E}_\pm$. It can be shown that Hopf bifurcation can occur from the $\mathrm{E}_\pm$ if the following condition holds:

$$p = p_{\mathrm{H}} \equiv \frac{b}{\frac{2(a+n)}{2m-(a+n)n} - \frac{a}{m}}, \quad \text{with} \quad \omega_{\mathrm{E}_\pm} = \sqrt{\tfrac{2am}{a+n}}, \tag{2.19}$$

at which the third eigenvalue is $-(a+n) < 0$. It is obvious that $am > 0$.

Now we investigate if Hopf bifurcations can occur simultaneously from the E_0 and $\mathrm{E}_\pm$. It is easy to see that a necessary condition for a Hopf bifurcation to

occur from the E_0 is $n = 0$ and then the characteristic polynomial become $\tilde{P}_{\mathrm{E}_0} = (\lambda + a)(\lambda^2 - m)$. With $n = 0$, the characteristic polynomial for the $\mathrm{E}_\pm$ becomes $P_{\mathrm{E}_\pm} = \lambda^3 + a\,\lambda^2 + \frac{2amp}{ap+bm}\,\lambda + 2am$. In order to have Hopf bifurcation from the $\mathrm{E}_\pm$, the condition $bm = 0$ must be satisfied, i.e., $b = 0$. Thus, $P_{\mathrm{E}_\pm}$ is reduced to $\tilde{P}_{\mathrm{E}_\pm} = (\lambda + a)(\lambda^2 + 2m)$. It follows from $\tilde{P}_{\mathrm{E}_0}$ and $\tilde{P}_{\mathrm{E}_\pm}$ that it is impossible to have Hopf bifurcations simultaneously from the E_0 and $\mathrm{E}_\pm$.

Summarizing the above results and discussions leads to the following theorem.

Theorem 2.2. *When $a > 0$, $m < 0$, system (1.1) can have Hopf bifurcation from the equilibrium E_0 at the critical point $n = 0$. When $am > 0$, $a + n > 0$, Hopf bifurcation can happen from the symmetric equilibria $\mathrm{E}_\pm$ at the critical point $p = p_{\mathrm{H}}$. It is not possible to have Hopf bifurcations arising simultaneously from the E_0 and $\mathrm{E}_\pm$.*

Local bifurcations in system (1.1) have been recently studied in detail by Zhou [29], obtaining some results. In particular it is shown that one limit cycle bifurcates from each of the two symmetric equilibria $\mathrm{E}_\pm$.

2.4. Limit cycle bifurcating from the E_0 of the extended Lorenz system (1.1)

We first consider Hopf bifurcation from the stable equilibrium E_0 when $a > 0$, $m < 0$ and $n > 0$. We have the following result.

Theorem 2.3. *When $a > 0$, $m < 0$, system (1.1) has a Hopf bifurcation from the equilibrium E_0 at the critical point $n = n_{\mathrm{H}} = 0$, and the Hopf bifurcation is supercritical (subcritical) if $b > 0$ ($b < 0$), leading to one stable (unstable) limit cycle near the E_0. For this case, no Hopf bifurcation can simultaneously appear from the equilibria $\mathrm{E}_\pm$.*

Proof. Hopf bifurcation occurs at the critical point $n = n_{\mathrm{H}} = 0$ at which the system has a pair of purely imaginary eigenvalues $\lambda_{1,2} = i\,\omega_{\mathrm{E}_0} = i\sqrt{-m}$ and one real eigenvalue $\lambda_3 = -a$. Introducing the transformation $y \to \sqrt{-m}\,y$ into (1.1) and then applying the Maple program [24] to the resulting system we obtain the following focus values:

$$
\begin{aligned}
v_1 &= \tfrac{bm}{4(a^2-4m)},\\
v_2 &= \tfrac{b}{16a(a^2-4m)^3}\left[bm(a^4-24ma^2+48m^2)+ap(a^2-4m)(a^2-16m)\right],\\
v_3 &= -\tfrac{b}{4096ma^2(a^2-4m)^5(a^2-16m)}\left[b^2m^2(2883584m^5-3306496m^4p^2+1241152m^3p^4\right.\\
&\quad -151856m^2p^6+9548mp^8-269p^{10})-2bmap(a^2-4m)(802816m^4-612864m^3a^2\\
&\quad +99152m^2a^4-8168ma^6+269a^8)+a^2p^2(a^2-4m)^2(256256m^3-59856m^2a^2\\
&\quad \left.+6936ma^4-269a^6)\right],\\
&\;\;\vdots
\end{aligned}
\tag{2.20}
$$

which show that when $b = 0$, $v_1 = v_2 = v_3 = \cdots = 0$. Thus, for $b \neq 0$, $v_1 \neq 0$, which implies that if a Hopf bifurcation occurs from the E_0, there is only one limit

cycle bifurcating from the E_0, and it is stable (unstable) for $b > 0$ ($b < 0$). It should be noted that the parameter p does not appear in the first focus value v_1, but in higher order focus values. □

2.5. Limit cycles bifurcating from the $E_\pm$ of the extended Lorenz system (1.1)

Now, we turn to Hopf bifurcation which emerges from the equilibria $E_\pm$. Since the two equilibria are symmetric with the z-axis, we only need to consider one of them. We have the following result.

Theorem 2.4. *When $am > 0$, $a + n > 0$, Hopf bifurcation can happen from the $E_\pm$ at the critical point $p = p_H$. The maximal number of small limit cycles near the E_+ or E_- can reach three with outer one being either stable or unstable. Thus, the total maximal number of limit cycles bifurcating from the symmetric equilibria $E_\pm$ is 6.*

Proof. Suppose $am > 0$ and $a + n > 0$. Then at the critical point $p = p_H$, Hopf bifurcation can occur from the $E_\pm$. Introducing the transformation:

$$\begin{pmatrix} x \\ y \\ z \end{pmatrix} = \begin{pmatrix} \sqrt{\frac{am}{ap+bm}} \\ 0 \\ \frac{bm}{ap+bm} \end{pmatrix} + T_2 \begin{pmatrix} u \\ v \\ w \end{pmatrix}, \tag{2.21}$$

where

$$T_2 = \begin{bmatrix} \frac{m\sqrt{a+n}}{\sqrt{2}\,m}\,\tilde{T} & \frac{m\sqrt{am}}{an}\,\tilde{T} & \frac{m\sqrt{(a+n)}}{\sqrt{2}\,a}\,\tilde{T} \\ \frac{\sqrt{2}\,m^2}{n\sqrt{a+n}}\,\tilde{T} & \frac{m\sqrt{am}}{n}\,\tilde{T} & \frac{m(a+n)\sqrt{a+n}}{\sqrt{2}\,a}\,\tilde{T} \\ 1 & 0 & 1 \end{bmatrix}, \tag{2.22}$$

with $\tilde{T} = \sqrt{an/[bm(2m + a^2 + an)]}$, into (1.1), we obtain the system:

$$\begin{aligned} \dot{u} &= \omega_{E_\pm}\, v + \textstyle\sum_{i+j+k=2}^{3} a_{ijk} u^i v^j w^k, \\ \dot{v} &= -\,\omega_{E_\pm}\, u + \textstyle\sum_{i+j+k=2}^{3} b_{ijk} u^i v^j w^k, \\ \dot{w} &= -\,(a+n)\, w + \textstyle\sum_{i+j+k=2}^{3} c_{ijk} u^i v^j w^k, \end{aligned} \tag{2.23}$$

where a_{ijk}, b_{ijk} and c_{ijk} are coefficients given in terms of a, m and n. Note that b does not appear in these expressions. Now applying the Maple program [24] to system (2.23) we obtain the following focus values:

$$v_1 = \frac{(a+n)m^2\,F_1}{8n^2(2m+a^2+an)^2[(a+n)^3+2am][(a+n)^3+8am]},$$

$$v_2 = \frac{(a+n)m^3\,F_2}{1152an^4(2m+a^2+an)^4[(a+n)^3+18am][(a+n)^3+2am]^3[(a+n)^3+8am]^3},$$

$$v_3 = \frac{(a+n)m^4\,F_3}{10616832a^2n^6(2m+a^2+an)^6[(a+n)^3+32am][(a+n)^3+18am]^2[(a+n)^3+2am]^5[(a+n)^3+8am]^5},$$

where

$$F_1 = 16an(3a+5n)\,m^3 + 2(a+n)(3a^3-27a^2n+5an^2+3n^3)\,m^2$$

$$- n(a+n)^2(39a^3+17a^2n+21an^2+3n^3)\,m - 2na^2(a+3n)(a+n)^4,$$

$$\begin{aligned}F_2 =& 2654208a^6(27a^2+104an+41n^2)\,m^{10}+36864a^5(a+n)(2349a^4+6134a^3n+13796a^2n^2\\ &+8314an^3+895n^4)m^9+512a^4(a+n)^2(56349a^6-260892a^5n+465033a^4n^2+963848a^3n^3\\ &+572295a^2n^4+131700an^5+20915n^6)\,m^8-64a^3(a+n)^3(13689a^8+3129822a^7n\\ &+4749174a^6n^2+2006a^5n^3-4883240a^4n^4-3867366a^3n^5-1080214a^2n^6-132686an^7\\ &-40881n^8)\,m^7-32a^2(a+n)^4(58779a^{10}+2799513a^9n+10139175a^8n^2+11938198a^7n^3\\ &+3813688a^6n^4-3403896a^5n^5-4294544a^4n^6-2108918a^3n^7-314283a^2n^8-15681an^9\\ &-6975n^{10})\,m^6-16a(a+n)^6(20682a^{11}+1405872a^{10}n+7828005a^9n^2+12922778a^8n^3\\ &+8412523a^7n^4+989849a^6n^5-1619143a^5n^6-1033043a^4n^7-510169a^3n^8-40925a^2n^9\\ &+2822an^{10}-371n^{11})m^5-8(a+n)^8(2835a^{12}+421623a^{11}n+2983311a^{10}n^2+7735180a^9n^3\\ &+8038629a^8n^4+3319151a^7n^5+100708a^6n^6-374829a^5n^7-40603a^4n^8-51862a^3n^9\\ &-2919a^2n^{10}+433an^{11}-9n^{12})\,m^4-4(a+n)^{11}(+135a^{11}+77202a^{10}n+406656a^9n^2\\ &+1508069a^8n^3+1853253a^7n^4+680325a^6n^5+109244a^5n^6-56790a^4n^7+13440a^3n^8\\ &-695a^2n^9-144an^{10}+9n^{11})\,m^3-2an(a+n)^{14}(8280a^8+6027a^7n+102829a^6n^2\\ &+245463a^5n^3+66072a^4n^4+21427a^3n^5-4059a^2n^6+717an^7+96n^8)\,m^2\\ &-a^2n(a+n)^{17}(360a^6-3123a^5n-3496a^4n^2+14928a^3n^3+2200a^2n^4+1113an^5+30n^6)m\\ &-2a^3n^2(a+n)^{20}(54a^3+95a^2n-45an^2-6n^3).\end{aligned}$$

Next, eliminating m from the two equations $F_1=0$ and $F_2=0$ yields a solution $m=m(a,n)=\frac{m_N(a,n)}{m_D(a,n)}\,a^2$, where

$$\begin{aligned}m_N =& -145118822400a^{39}+8420297074713a^{38}n+1937334345180876a^{37}n^2\\ &+136155571646782572a^{36}n^3+3194798805759399984a^{35}n^4+35966616792047795259a^{34}n^5\\ &+221922136598323411602a^{33}n^6+753875689130289285408a^{32}n^7\\ &+1036143752291928742968a^{31}n^8-1505852094040225275492a^{30}n^9\\ &-7521991071123630239280a^{29}n^{10}-8211091338516468330576a^{28}n^{11}\\ &+5660913430498046904648a^{27}n^{12}+2397097062256468643168 4a^{26}n^{13}\\ &+2556439329389678039628 0a^{25}n^{14}+6380816427649337371056a^{24}n^{15}\\ &-1624744968143627121492 0a^{23}n^{16}-2478444020605522185474 6a^{22}n^{17}\\ &-1769766988694930152005 6a^{21}n^{18}-5410371960997707843128a^{20}n^{19}\\ &+2826476114555371783784a^{19}n^{20}+5041918024385859760450a^{18}n^{21}\\ &+3842602497120806887244a^{17}n^{22}+2029417648468590252752a^{16}n^{23}\\ &+817423705912582945640a^{15}n^{24}+256168487662741448508a^{14}n^{25}\\ &+599016346927866389 28a^{13}n^{26}+834982077236049758 4a^{12}n^{27}\\ &-483850144879369448a^{11}n^{28}-617779803879041660a^{10}n^{29}\\ &-134169454772069576a^9n^{30}+7248773523375824a^8n^{31}\\ &+113189552575748 24a^7n^{32}+293500068402282 5a^6n^{33}+360376751146188a^5n^{34}\\ &+14796815063148a^4n^{35}-1381381134072a^3n^{36}-177186390981a^2n^{37}\\ &-5150585614an^{38}+45632400n^{39},\end{aligned}$$

$$
\begin{aligned}
m_D =& 676674967950a^{39} - 360610005790854a^{38}n - 46790439207463134a^{37}n^2 \\
&- 2538421275417013008a^{36}n^3 - 482236418209694236 56a^{35}n^4 \\
&- 413330520617120880792a^{34}n^5 - 1692478899149910020658a^{33}n^6 \\
&- 2439292211384651284140a^{32}n^7 + 5495797103327313434388a^{31}n^8 \\
&+ 1888474868577419416887 6a^{30}n^9 + 6357144596804918851860a^{29}n^{10} \\
&- 2677835893184592223676 4a^{28}n^{11} - 4049951241281830284330 0a^{27}n^{12} \\
&- 1885892578576102412406 0a^{26}n^{13} + 1573386729432892580566 8a^{25}n^{14} \\
&+ 3255391376737758717800 4a^{24}n^{15} + 2472948218361598904961 6a^{23}n^{16} \\
&+ 7853263895059354960704a^{22}n^{17} - 3568017877172945296584a^{21}n^{18} \\
&- 6342834624755658568556a^{20}n^{19} - 4519243537029378496868a^{19}n^{20} \\
&- 2215427028162452220828a^{18}n^{21} - 8765902472207495405 44a^{17}n^{22} \\
&- 3241551986304638713 80a^{16}n^{23} - 1206348490420193817 16a^{15}n^{24} \\
&- 3830180304573443447 6a^{14}n^{25} - 5803329993294537460a^{13}n^{26} \\
&+ 2400862034147721580a^{12}n^{27} + 196808463457452430 8a^{11}n^{28} \\
&+ 604420369610938924a^{10}n^{29} + 54352478959614300a^{9}n^{30} \\
&- 26945906948502052a^{8}n^{31} - 11971332115482078a^{7}n^{32} - 2278682250361402a^{6}n^{33} \\
&- 217136364420986a^{5}n^{34} - 4630424296084a^{4}n^{35} + 1081216070812a^{3}n^{36} \\
&+ 100863436964a^{2}n^{37} + 2547730482an^{38} - 20078256n^{39},
\end{aligned}
$$

and a resultant:

$$\mathrm{R}_{12} = an(a^2 - n^2)(9a^2 - n^2)\,\mathrm{R}_{12\mathrm{a}}(a, n),$$

where

$$
\begin{aligned}
\mathrm{R}_{12\mathrm{a}} =& 6643012500a^{39} + 680229717750a^{38}n + 27941732823690a^{37}n^2 \\
&+ 243031205836926a^{36}n^3 - 3870453629582919a^{35}n^4 - 113872116973144644a^{34}n^5 \\
&- 1455977799249345657a^{33}n^6 - 11758763677939125183a^{32}n^7 \\
&- 6037998639914848653 9a^{31}n^8 - 1855623272616372294 99a^{30}n^9 \\
&- 2559208682194601211 81a^{29}n^{10} + 1700961665216433591 51a^{28}n^{11} \\
&+ 8668015803548538833 07a^{27}n^{12} - 4399244277936662790 81a^{26}n^{13} \\
&- 5677778080742194310427a^{25}n^{14} - 1138940641436681362 6071a^{24}n^{15} \\
&- 1035594855198055759 3491a^{23}n^{16} - 6301789301853497251 03a^{22}n^{17} \\
&+ 1083637357623110604 6695a^{21}n^{18} + 1552958774482091422 4779a^{20}n^{19} \\
&+ 1164403466482592368 6957a^{19}n^{20} + 4032060514054361867623a^{18}n^{21} \\
&- 1739954990466126836941a^{17}n^{22} - 3684240222100387596117a^{16}n^{23} \\
&- 3018923218712379290201a^{15}n^{24} - 1664487129593507485145a^{14}n^{25} \\
&- 6767390151366318071 83a^{13}n^{26} - 2061714926830057770 99a^{12}n^{27} \\
&- 4607705028531523567a^{11}n^{28} - 7017422324887267571a^{10}n^{29} \\
&- 549115344386489281a^{9}n^{30} + 322757823781927 31a^{8}n^{31} \\
&+ 153051581353648 35a^{7}n^{32} + 1973401335496141a^{6}n^{33} \\
&+ 107944455360187a^{5}n^{34} - 2587735411437a^{4}n^{35} - 775708992674a^{3}n^{36}
\end{aligned}
$$

$$-44282118919a^2n^{37}-765584094an^{38}+6692752n^{39},$$

which is a 39th-degree homogeneous polynomial in a and n. It is easy to show that setting $n(a^2-n^2)(9a^2-n^2)=0$ yields the $\mathrm{E}_\pm$ being saddle points. Therefore, it is not possible to find solutions such that $v_1=v_2=v_3=0$, and so four limit cycles can not exist. The next best possibility is to find three limit cycles, which can be obtained by solving the equation $\mathrm{R}_{12\mathrm{a}}=0$. Letting $n=Na$ and then solving $\mathrm{R}_{12\mathrm{a}}=0$ for $N\neq 0$ yields 11 real solutions, and then using the solution $m(a,n)$ we obtain the following 11 solutions:

$$\begin{aligned}(m,n)=&(0.007147\cdots a^2,\ -0.570923\cdots a),\quad (0.021999\cdots a^2,\ -1.392097\cdots a),\\ &(0.804329\cdots a^2,\ -2.361528\cdots a),\quad (1.922924\cdots a^2,\ 0.961226\cdots a),\\ &(12829.627127\cdots a^2,\ 160.256166\cdots a),\\ &(-300.180082\cdots a^2,\ 13.507367\cdots a),\quad (-2.918811\cdots a^2,-15.268853\cdots a),\\ &(-1.323394\cdots a^2,\ 8.439914\cdots a),\quad (-0.569859\cdots a^2,\ 1.250380\cdots a),\\ &(-0.370621\cdots a^2,\ -0.453226\cdots a),\quad (-0.065623\cdots a^2,\ 0.056199\cdots a).\end{aligned}$$

It is easy to use the conditions $am>0$ and $a+n>0$ to verify that only the 4th, 5th and 7th solutions are feasible solutions, that is, the feasible three solutions are the following ones, satisfying $v_1=v_2=0$:

$$\begin{aligned}a>0\colon\ &\begin{cases}\mathrm{S}_1=(1.922924\cdots a^2,\quad 0.961226\cdots a):\ v_3=\quad 0.0178165052\cdots a>0,\\ \mathrm{S}_2=(12829.62\cdots a^2,\quad 160.2561\cdots a):\ v_3=-3.1288470830\cdots a<0,\end{cases}\\ a<0\colon\ &\mathrm{S}_3=(-2.9188\cdots a^2,\ -15.26885\cdots a):\quad v_3=\quad 0.0000008598\cdots a<0.\end{aligned}\tag{2.24}$$

The above results indicate that the stability of the three limit cycles can be different since the outer one can be either stable or unstable. It follows from (2.18) that the first solution S_1 belongs to Case II, the second solution S_2 belongs to Case I, and the last solution S_3 belongs to Case III. Further, a direct calculation shows that

$$\frac{\partial(v_1,v_2)}{\partial(m,n)}=\left\{\begin{array}{l}\dfrac{0.1597421584\cdots}{a}\times 10^{-7},\text{ for solution }\mathrm{S}_1\\ \dfrac{0.1245322791\cdots}{-a}\times 10^{-5},\text{ for solution }\mathrm{S}_2\\ \dfrac{0.1739537197\cdots}{a}\times 10^{-8},\text{ for solution }\mathrm{S}_3\end{array}\right\}\neq 0,$$

which implies that three limit cycles can be obtained near each of the two symmetric equilibria $\mathrm{E}_\pm$ by perturbing the parameters p, m and n, while a and b can be chosen arbitrarily according to the conditions given in (2.18).

The proof of Theorem 2.4 is complete. □

3. Simulation of limit cycles

In this section, we present several numerical examples to illustrate the theoretical results obtained in previous sections for the standard Lorenz system (1.3) and the extended Lorenz system (1.1). The simulations are obtained by using the Matlab software package with ODE45 (2017 version).

3.1. Two unstable limit cycles near the $C_\pm$ of the Lorenz system (1.3)

We take the parameter values, which are usually used in the literature for finding the butterfly chaotic attractor of system (1.3) (e.g., see [3]), given by $\sigma = 10$, $r = \frac{8}{3}$, for which $\rho_H = 24\frac{14}{19}$. At this critical point, the non-zero equilibria are given by

$$C_\pm : \quad (X, Y, Z) = (\pm 7.956019458,\ \pm 7.956019458,\ 23.73684211).$$

For the above critical parameter values, the first focus value is $v_1 \approx 0.0010804123$. In order to find the small-amplitude (unstable) limit cycle, we need to find v_0 such that $0 < -v_0 \ll v_1$. v_0 can be obtained from a linear analysis, which is actually the read part of the complex conjugate eigenvalue of the Jacobian of system (1.3). To achieve this, we perturb ρ from ρ_H to $\rho = \rho_H - \frac{1}{100} = \frac{46981}{1900}$. Then, a direct computation shows that the eigenvalues of the Jacobian of system (1.3) are

$$\lambda_{1,2} = -0.0003022716 \pm 9.6227153375\, i \quad \text{and} \quad \lambda_3 = -13.6660621236,$$

showing that $v_0 = -0.0003022716$. Therefore, the truncated normal form up to third order, given by

$$\dot{r} = v_0\, r + v_1\, r^3 = -0.0003022716\, r + 0.0010804123\, r^3,$$

has a positive solution, $r = 0.5289369236$, which approximates the amplitude of the (unstable) limit cycle. The simulation is shown in Figure 1, where two trajectories starting from two different initial conditions chosen near the equilibria $C_\pm$, diverge to the well-known Lorenz butterfly chaotic attractor.

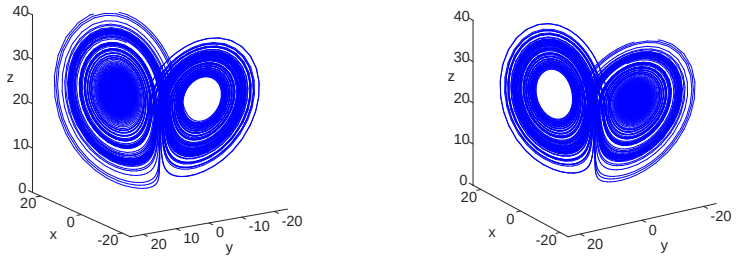

(a) $(X, Y, Z) = (7, 956, 7.956, 23.7368)$ (b) $(X, Y, Z) = (-7, 956, -7.956, 23.7368)$

Figure 1. Simulation of the Lorenz system (1.3), showing coexistence of the unstable limit cycles around the symmetric equilibria $C_\pm$ and the butterfly chaotic attractor, for $\sigma = 10$, $r = \frac{8}{3}$ and $\rho = \frac{46981}{1900}$ with the initial points.

It can be seen from Figure 1 that the trajectory starting from the initial point near the equilibrium C_+ frequently visits the area near the unstable limit cycle around the equilibrium C_-, as shown in Figure 1(a). Similar situation happens when the initial point is chosen near the equilibrium C_-. This shows coexistence of unstable limit cycles and the butterfly chaotic attractor.

3.2. Limit cycle bifurcations in the extended Lorenz system (1.1)

We now turn to the extended Lorenz system (1.1). First, we consider the limit cycle bifurcation from the E_0 (the origin), and then from the symmetric equilibria $E_\pm$.

3.2.1. One limit cycle around the E_0

It has been shown that only one limit cycle exists near the E_0 due to Hopf bifurcation and its stability depends upon the sign of b. We choose $m = -1$ and $a = 1$. Then choosing $b = \frac{1}{2}$, we obtain $v_1 = -\frac{1}{40}$, indicating that the limit cycle is stable. In order to have this small-amplitude limit cycle, we need $0 < v_0 \ll -v_1$. Similar to the discussion given in Section 3.1 for the Lorenz system (1.3), we may let $n = -\frac{1}{20}$, which yields the eigenvalues of the linearized system as

$$\lambda_{1,2} = \frac{1}{40} \pm i\,\frac{\sqrt{599}}{40}, \quad \lambda_3 = -1,$$

and so $v_0 = \frac{1}{40}$. Thus, the truncated normal form is

$$\dot{r} = v_0\, r + v_1\, r^3 = \frac{1}{40}\, r - \frac{1}{40}\, r^3$$

which gives the approximation of the stable limit cycle $r = 1$, as shown in Figure 2(a).

If we change b from $\frac{1}{2}$ to $-\frac{1}{2}$, then we obtain $v_1 = \frac{1}{40}$. Further, let $n = \frac{1}{20}$. Then, $v_0 = -\frac{1}{40}$, yielding the same approximation of limit cycle $r = 1$. However, this limit cycle is unstable, as shown in Figure 2(b). It is noted that the unstable limit cycle, shown in Figure 2(b) with negative z, seems symmetric to the stable one, shown in Figure 2(a) with positive z. Actually, if we change $(x, y, z) \to (-x, -y, -z)$ and $(n, b) \to (-n, -b)$, we obtain the following system:

$$\begin{aligned} \dot{x} &= y, \\ \dot{y} &= m\, x + n\, y + m\, xz - p\, x^3, \\ \dot{z} &= -\, a\, z + b\, x^2. \end{aligned} \tag{3.1}$$

System (3.1) has an unstable limit cycle, as shown in Figure 2(c), which is exactly symmetric to the one given in Figure 2(b). The attracting region of the stable equilibrium $(0, 0, 0)$ is actually quite large. When the initial point is chosen as $(x, y, z) = (-0.9, -2, -100)$, as shown in Figure 2(d), the trajectory converges to the origin via the manifold containing the unstable limit cycle. It is seen from Figures 2(b) and (d) that these two diagrams show almost exactly the same trajectory near the origin, but the one given in Figure 2(d) has more part on the manifold since the initial point is much far away than the one depicted in Figure 2(b). Also note that the equilibria $E_\pm$ do not exist for the above chosen parameter values. Therefore, for these parameter values, if the initial point is not chosen from the attracting region, the trajectory will diverge to infinity.

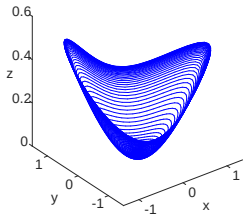

(a) for system (1.1) with $n = -\frac{1}{20}$ and $b = \frac{1}{2}$ and the initial point $(x, y, z) = (0.01, 0.01, 0.01)$, a stable limit cycle exists

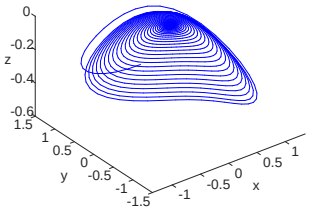

(b) for system (1.1) with $n = \frac{1}{20}$ and $b = -\frac{1}{2}$ and the initial point $(x, y, z) = (-0.5, -1.3, 0.2)$, an unstable limit cycle appears

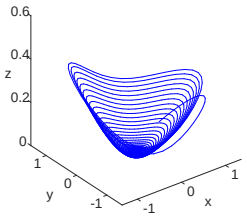

(c) for system (3.1) which is symmetric with system (1.1) under $(x, y, z) \to (-x, -y, -z)$ and $(n, b) \to (-n, -b)$, an unstable limit cycle exists, which is symmetric with the one shown in (b)

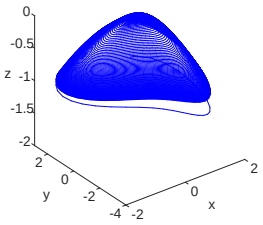

(d) for system (1.1) with $n = \frac{1}{20}$ and $b = -\frac{1}{2}$ and the initial point $(x, y, z) = (-0.9, -2, -100)$, an unstable limit cycle appears

Figure 2. Simulation of the extended Lorenz system when $m = -1$ and $p = a = 1$.

3.2.2. Six limit cycles around the $\mathrm{E}_{\pm}$

Finally, we present simulation for the six limit cycles, with three around each of the equilibria $\mathrm{E}_{\pm}$. According to the solutions classified in (2.24), we have three sets of solutions. We will give one simulation for each case.

Case S_1. We take $a = 1$, for which $v_3 = 0.0178165052\cdots > 0$ and $v_0 = v_1 = v_2 = 0$. This indicates that the largest small-amplitude limit cycle is unstable. Then, we perturb $(m, n) = (1.9229244660, 0.96122637340)$ to $(m, n) = (1.8858259631, 0.9423396437)$ under which $0 < v_1 \ll -v_2 \ll v_3$. More precisely, we obtain the following new focus values:

$$v_1 \approx 0.0000106149, \quad v_2 \approx -0.0009994525, \quad v_3 \approx 0.0164962448,$$
$$v_4 \approx 0.0564177682, \quad v_5 \approx 0.1683022855.$$

Further, without loss of generality, we set $b = 0.5$. Under the above chosen parameter values, we finally perturb p from $p_H = 0.3399531456$ to $p = 0.3399531956$ so that $v_0 \approx -0.0000000184$ for which the equilibria $\mathrm{E}_{\pm} = (\pm 1.2124396423, 0, 0.7350049431)$. Then, the truncated 7th-order normal form is given by

$$\begin{aligned}\dot{r} &= v_0 r + v_1 r^3 + v_2 r^5 + v_3 r^7 \\ &= -0.0000000184r + 0.0000106149r^3 - 0.0009994525r^5 + 0.0164962448r^7,\end{aligned}$$

which has three positive roots:

$$r_1 \approx 0.046424, \quad r_2 \approx 0.104346, \quad r_3 \approx 0.217934.$$

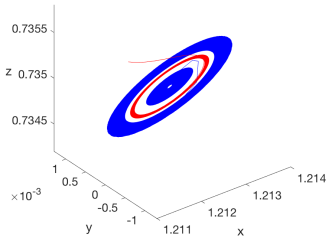

(a) from the initial points: $(x, y, z) = (1.2124, 0, 0.735)$ (trajectory in blue color) and $(x, y, z) = (1.2124, 0.001, 0.735)$ (trajectory in red color)

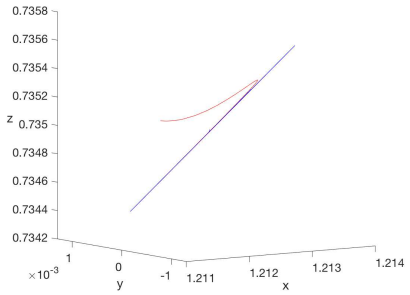

(b) a different projection of (a) showing an almost plane shape of the center manifold embedding the limit cycles

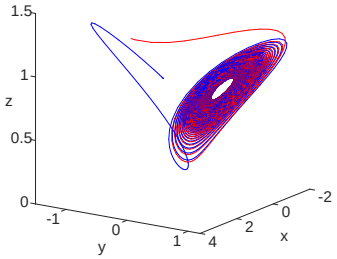

(c) two trajectories starting from the initial points: $(x, y, z) = (2, 0, 1)$ and $(-2, 0, -4)$ converge to the stable limit cycle

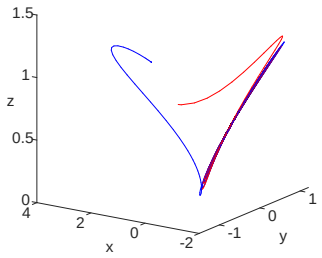

(d) a different projection of (c) showing an almost plane shape of the center manifold

Figure 3. Simulated trajectories of the extended Lorenz system when $a = 1$, $m = 1.8858259631$, $n = 0.9423396437$, $b = 0.5$ and $p = 0.3399531956$, showing convergence to the stable limit cycle.

In order to see if higher order focus values affect the solution of the roots, we add two additional higher-order terms to the above truncated normal form to obtain the 11th-order normal form:

$$\begin{aligned}\dot{r} &= v_0 r + v_1 r^3 + v_2 r^5 + v_3 r^7 + v_4 r^9 + v_5 r^{11} \\ &= -0.0000000184r + 0.0000106149r^3 - 0.0009994525r^5 + 0.0164962448r^7 \\ &\quad + 0.0564177682r^9 + 0.1683022855r^{11},\end{aligned}$$

which again has three positive roots:

$$r_1 \approx 0.046360, \quad r_2 \approx 0.105140, \quad r_3 \approx 0.197517.$$

It is seen that these three roots are quite close to that obtained from the 7th-order normal form, indicating that these approximations of the amplitudes of the three small-amplitude limit cycles are robust.

Simulation for this case are depicted in Figure 3, which only shows the limit cycles around the equilibrium E_+ since E_- is symmetric to E_+. In Figure 3(a), two very close initial points: $(x, y, z) = (1.2124, 0, 0.735)$ and $(1.2124, 0.0001, 0.735)$ are chosen to perform the simulation. It is seen from Figure 3(a) that the trajectory starting from the second initial point (in red color) converge to the stable limit cycle, while the trajectory starting from the first initial point (in blue color) first approaches the stable limit cycle, and then jumps to outside of the stable limit cycle and continues to expand out. It is expected that the blue trajectory inside the red trajectory should approach the red trajectory (the stable limit cycle), but the sudden jump may be due to numerical accumulation error. However, the outside blue trajectory shows an unstable limit cycle which exists between the red trajectory and the outside blue trajectory. Since E_+ is stable, there must exist an unstable limit cycle between the E_+ and the stable limit cycle, which is located on the center manifold and very close to the equilibrium E_+. A projection taken in a difference angle, depicted in Figure 3(b), shows that the center manifold near the equilibrium E_+ is almost a plane. Since higher-order focus values are positive (verified up to the term r^{27}), there must exist an unstable limit cycle outside the stable one. Moreover, two trajectories shown in Figures 3(c) and (d), starting respectively from the initial points: $(x, y, z) = (2, 0, 1)$ and $(-2, 0, -4)$, indicate that other trajectories converge to the stable limit cycle.

Case S_2. We choose $a = 0.005$, which gives $v_3 = -0.0156442354\cdots < 0$ and $v_0 = v_1 = v_2 = 0$. This implies that the largest small-amplitude limit cycle is stable. Then, we perturb $(m, n) = (0.3207406782, 0.8012808319)$ to $(m, n) = (0.1658993054, 0.5762527391)$ for which the focus values become

$$v_1 \approx -0.4253389437\times10^{-5},\ v_2 \approx 0.4413506704\times10^{-3},\ v_3 \approx -0.6084976817\times10^{-2},$$
$$v_4 \approx -0.1158033372, \qquad v_5 \approx -1.541745839.$$

Again we set $b = 0.5$. Under these chosen parameter values, we finally perturb p from $p_H = -0.0013546668$ to $p = -0.0013551358$ so that $v_0 \approx 0.8002492701\times10^{-8}$ for which the equilibria $E_\pm = (\pm0.1000040844, 0, 1.0000816909)$. Then, the truncated 7th-order normal form is given by

$$\begin{aligned}\dot r =& v_0 r + v_1 r^3 + v_2 r^5 + v_3 r^7 = 0.8002492701\times10^{-8} r - 0.4253389437\times10^{-5} r^3\\ &+ 0.4413506704\times10^{-3} r^5 - 0.6084976817\times10^{-2} r^7,\end{aligned}$$

which has three positive roots:

$$r_1 \approx 0.050150, \quad r_2 \approx 0.092197, \quad r_3 \approx 0.248024.$$

When higher order focus values v_4 and v_5 are added to the above truncated normal form, we obtain

$$\begin{aligned}\dot r =& v_0 r + v_1 r^3 + v_2 r^5 + v_3 r^7 + v_4 r^9 + v_5 r^{11}\\ =& 0.8002492701\times10^{-8} r - 0.4253389437\times10^{-5} r^3\\ &+ 0.4413506704\times10^{-3} r^5 - 0.6084976817\times10^{-2} r^7 - 0.1158033372 r^9\\ &- 1.5417458391 r^{11},\end{aligned}$$

which again has three positive roots:

$$r_1 \approx 0.050128, \quad r_2 \approx 0.094327, \quad r_3 \approx 0.168516.$$

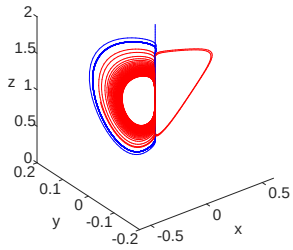

(a) starting from the two initial points: $(x, y, z) = (-0.01, -0.001, 0.7984027)$ and $(x, y, z) = (-2, 0, 1)$, converging to two stable limit cycles, with the smaller one in red and larger one in blue

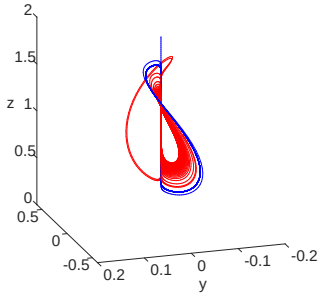

(b) a different projection of the phase portrait in (a), showing the shape of the center manifold embedding the limit cycles

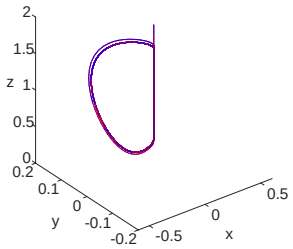

(c) trajectories starting from $(x, y, z) = (2, 0, -3)$ and $(-3, 1, 3)$ converge to the larger stable limit cycle

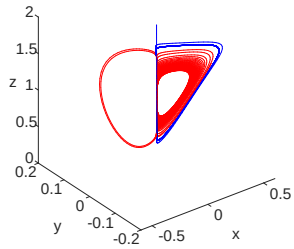

(d) a symmetric phase portrait of that in (a) using the initial points: $(x, y, z) = (0.01, 0.001, 0.7984027)$ and $(x, y, z) = (2, 0, 1)$

Figure 4. Simulated trajectories of the extended Lorenz system (1.1) when $a = 0.005$, $m = 0.1658993054$, $n = 0.5762527391$, $b = 0.5$ and $p = -0.0013551358$.

It is seen that the first two roots are very close to that obtained from the 7th-order normal form, while the third one is slightly less than the one from the 7th-order normal form, indicating that these approximations of the amplitudes of the three small-amplitude limit cycles are robust.

Simulations for this case are depicted in Figure 4, which show two stable limit cycles enclosing the equilibria $E_{\pm}$. The trajectory starting from the initial point, $(x, y, z) = (-0.01, -0.001, 0.7984027)$, converges to the smaller limit cycle (in red), while the one starting from the initial point, $(x, y, z) = (-2, 0, 1)$, converges to the larger stable limit cycle (in blue). The center manifold embedding the limit cycles is depicted in Figure 4(b). There exists an unstable limit cycle between the two stable limit cycles, and the equilibria $E_{\pm}$ are unstable. Figure 4(c) shows that trajectories starting from the initial points far away from the equilibria converge to the larger stable limit cycle. Figure 4(d) shows a phase portrait symmetric to that in (a) when the symmetric initial points, $(x, y, z) = (0.01, 0.001, 0.7984027)$ and $(2, 0, 1)$ are used.

Case S_3. For this case, $a<0$. We have $v_3 = 0.8598713267\cdots\times10^{-6}\,a < 0$ ($a < 0$) and $v_0 = v_1 = v_2 = 0$. This implies that the largest small-amplitude limit cycle is stable. Then, we perturb $(m, n) = (-2.9188113835\,a^2, -15.2688532498\,a)$ to

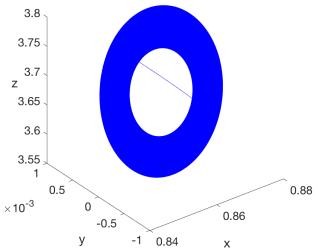

(a) converging to the smaller stable limit cycle

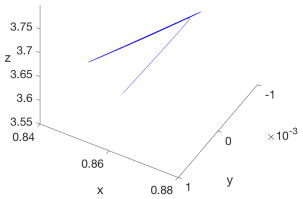

(b) a different projection of the phase portrait in (a), showing the almost plane shape of the center manifold

Figure 5. A simulated trajectory of the extended Lorenz system (1.1) when $a = -0.1$, $m = 0.8858259631$, $n = 0.9423396437$, $b = -0.5$ and $p = 0.3399531956$ with the initial point: $(x, y, z) = 0.8587, 0.01, 3.6871)$.

$(m, n) = (-2.9183094335\,a^2,\ -15.2745213540\,a)$ for which the focus values become

$$v_1 \approx 0.1717405600\times10^{-9}\,a, \quad v_2 \approx -0.2574566232\times10^{-7}\,a,$$
$$v_3 \approx 0.8569028948\times10^{-6}\,a, \quad v_4 \approx 0.4534920741\times10^{-7}\,a,$$
$$v_5 \approx -0.8436340643\times10^{-9}\,a.$$

For this case, it needs $b < 0$ (see Eq. (2.18)). We choose $b = -0.5$. Under the chosen parameter values, we finally perturb p from $p_H = -1.06340562335859\,a$ to $p = -1.06340562335853\,a$ so that $v_0 \approx 0.1140543640 \times 10^{-12}\,a < 0$ for which the equilibria $\mathrm{E}_\pm = (\pm2.7155368789\sqrt{-a},\ 0,\ 3.6870702704)$. Then, the truncated 7th-order normal form is given by

$$\begin{aligned}\dot r =& v_0 r + v_1 r^3 + v_2 r^5 + v_3 r^7 = -ar\big[0.1140543640\times10^{-12} - 0.1717405600\times10^{-9} r^2\\ &+ 0.2574566232\times10^{-7}\,r^4 - 0.8569028948\times10^{-6}\,r^6\big],\end{aligned}$$

which has three positive roots:

$$r_1 \approx 0.027301, \quad r_2 \approx 0.093005, \quad r_3 \approx 0.143711.$$

When higher order focus values v_4 and v_5 are added to the above truncated normal form, we obtain

$$\begin{aligned}\dot r =& v_0 r + v_1 r^3 + v_2 r^5 + v_3 r^7 + v_4 r^9 + v_5 r^{11}\\ =& -ar\big[0.1140543640\times10^{-12} - 0.1717405600\times10^{-9} r^2 + 0.2574566232\times10^{-7} r^4\\ &- 0.8569028948\times10^{-6} r^6 - 0.4427134796\times10^{-7} r^8 - 0.2034258917\times10^{-8} r^{10}\big],\end{aligned}$$

which again has three positive roots:

$$r_1 \approx 0.027301, \quad r_2 \approx 0.093005, \quad r_3 \approx 0.143574.$$

It is seen that these three roots are almost the same as that obtained from the 7th-order normal form, indicating that these approximations of the amplitudes of the three small-amplitude limit cycles are robust.

Simulation showing the smaller stable limit cycle is depicted in Figure 5(a). The trajectory starts from an initial point near the E_+: $(x, y, z) = (0.8587, 0.01, 3.6871)$. It is seen from Figure 5(b) that the center manifold is almost a plane, like Case S_1, as shown in Figure 3(b). However, for this case, it is hard to simulate the larger stable limit cycle, even though higher-order focus values (verified up to the term r^{31}) have the same negative sign of v_3. Many initial points are chosen but failed to find the larger stable limit cycle. For example, let the initial point be $(x, y, z) = (x_0, 0, 4)$. When $|x_0| \leq 1.051$, all trajectories converge to the smaller stable limit cycle; while when $|x_0) > 1.051$, all trajectories diverge to infinity. This may perhaps be caused by $a < 0$ for which the invariant manifold (the z-axis) is unstable, while it is an stable invariant manifold for the cases S_1 and S_2.

4. Conclusion

In this paper, we have considered an extended Lorenz system and applied normal form theory to study bifurcation of limit cycles due to Hopf bifurcation. It is shown that either one limit cycle (which may be stable or unstable) can bifurcate from the trivial equilibrium (the origin), or six limit cycles bifurcate from two symmetric equilibria. It is not possible to have Hopf bifurcations simultaneously from the trivial and the two symmetric equilibria. For comparison, we also show that the classical Lorenz system does not have Hopf bifurcation from the trivial equilibrium, and only one unstable limit cycle can occur from each of the two symmetric equilibria due to Hopf bifurcation.

Acknowledgements

This research was partially supported by the Natural Science and Engineering Research Council of Canada (NSERC No. R2686A02), the National Natural Science Foundation of China (NNSF No. 11431008), and China Postdoctoral Science Foundation (CPSF No. 2014M551873).

References

[1] L. S. Chen and M. S. Wang, *The relative position, and the number, of limit cycles of a quadratic differential system*, Acta. Math. Sinica, 1979, 22, 751–58.

[2] C. Du, Y. Liu and W. Huang, *A class of three-dimensional quadratic systems with ten limit cycles*, Int. J. Bifur. Chaos, 2016, 26, 1650149.

[3] J. Guckenheimer and P. Holmes, *Nonlinear Oscilla- tions, Dynamical Systems, and Bifurcations of Vector Fields (4th ed.)*, (New York: Springer-Verlag), 1993.

[4] M. Han, *Bifurcation of limit cycles of planar systems, Handbook of Differential Equations, Ordinary Differential Equations*, Vol. 3 (Eds. A. Canada, P. Drabek and A. Fonda), Elsevier, 2006.

[5] M. Han and P. Yu, *Normal Forms, Melnikov Functions, and Bifurcation of Limit Cycles*, London: Springer, 2012.

[6] D. Hilbert, *Mathematical problems*, (M. Newton, Transl.) Bull. Am. Math., 1902, 8, 437–79.

[7] E. Hopf, *Abzweigung einer periodischen Losung von stationaren Losung einers differential-systems*, *Ber. Math. Phys. Kl. Sachs Acad. Wiss. Leipzig*, 1942, 94, 1–22; and Ber. Math. Phys. Kl. Sachs Acad. Wiss. Leipzig Math.-Nat. Kl., 95, 3–22.

[8] C. Li and G. Chen, *A note on Hopf bifurcation in Chen's system*, Int. J. Bifur. Chaos, 2003, 13, 1609–15.

[9] C. Li, C. Liu and J. Yang, *A cubic system with thirteen limit cycles*, J. Diff. Eqns., 2009, 246, 3609–19.

[10] J. Li, *Hilbert's 16th problem and bifurcations of planar polynomial vector fields*, Int. J. Bifur. Chaos, 2003, 13, 47–106.

[11] J. Li and Y. Liu, *New results on the study of Z_q-equivariant planar polynomial vector fields*, Qual. Theory Dyn. Syst., 2010, 9(1–2), 167–219.

[12] L. Liu, O. Aybar, V. G. Romanovski and W. Zhang, *Identifying weak foci and centers in the Maxwell-Bloch system*£ J. Math. Anal. Appl., 2015, 430, 549–71.

[13] J. H. Lü, G. R. Chen, D. Z. Cheng and S. Celikovsky, *Bridge the gap between the Lorenz system and the Chen system*, Int. J. Bifur. Chaos, 2002, 12, 2917–26.

[14] J. H. Lü, G. R. Chen and S. Zhang, *Dynamical analysis of a new chaotic attractor,* Int. J. Bifur. Chaos, 2002, 12, 1001–15.

[15] J. E. Marsden and M. McCracken, *The Hopf bifurcation and Its Applications* (New York: Springer-Verlag), 1976.

[16] I. Ovsyannikov and D. Turaev, *Lorenz attractors and shilnikov criterion*, ArXiv preprint, arXiv:1508.07565 [v2], 2016.

[17] J. Pade, A. Rauh and G. Tsarouhas, *Analytical investigation of the Hopf bifurcation in the Lorenz model*, Phys. Lett. A, 1986, 115, 93–96.

[18] S. Shi, *An example for quadratic systems (E_2) to have at least four limit cycles,* Sci. Sinica, 1979, 11, 1051–56 (in Chinese).

[19] S. Shi£ *A concrete example of the existence of four limit cycles for plane quadratic systems,* Sci. Sinica, 1980, 23, 153–58.

[20] S. Smale, *Mathematical problems for the next century*, Math. Intell., 1988, 20, 7–15.

[21] Y. Tian and P. Yu, *An explicit recursive formula for computing the normal form and center manifold of n-dimensional differential systems associated with Hopf bifurcation,* Int. J. Bifur. Chaos, 2013, 23, 1350104 (18 pages).

[22] Y. Tian and P. Yu, *An explicit recursive formula for computing the normal forms associated with semisimple cases,* Commun. Nonlinear Sci. Numer. Simulat., 2014, 19, 2294–308.

[23] Q. Wang, W. Huang and J. Feng, *Multiple limit cycles and centers on center manifolds for Lorenz system*, Appl. Math. Comput., 2014, 238, 281–88.

[24] P. Yu, *Computation of normal forms via a perturbation technique*, J. Sound and Vib., 1998, 211, 19–38.

[25] P. Yu and M. Han, *Small limit cycles bifurcating from fine focus points in cubic-order Z_2-equivariant vector fields,* Chaos, Solitons Fractals, 2005, 24, 329–48.

[26] P. Yu and M. Han, *Ten limit cycles around a center-type singular point in a 3-d quadratic system with quadratic perturbation*, Appl. Math. Lett., 2015, 44, 17–20.

[27] Y. Yu and S. Zhang, *Hopf bifurcation in the Lü system*, Chaos Solitons Fractals, 2003, 17, 901–06.

[28] Y. Yu and S. Zhang, *Hopf bifurcation analysis of the Lü system*, Chaos Solitons Fractals, 2004, 21, 1215–20.

[29] Z. Zhou, *Local Bifurcations for Several Types of Higher-Dimensional Systems*, PhD Thesis, Shanghai: Shanghai Normal University, 2017.